

Investigation of ablation mechanism for laser-based lithotripsy

By Agon Kokaj

Investigation of ablation mechanism for laser-based lithotripsy

Agon Kokaj¹, Haxhi Kamberi¹, Muhamet Kadrija^{1,2}

¹University “Fehmi Agani”, Gjakove, Kosova

²Department of Public Health and Infectious Diseases, Sapienza University, Rome, Italy

Corresponding author:

Muhamet Kadrija

E-mail: muhamet.kadrija@uni-gjk.org

Abstract:

The formation of stones in the organs of the human body, such as in the kidneys or in the gall bladder, can cause serious health problems. Conventional surgery has been applied for extraction or ultrasound to destroy stones in human organs. However, laser lithotripsy, which is based on the delivery of laser energy from an optical fiber to a stone by optical fiber, has been shown to be a powerful and in many cases very useful technique for eliminating unwanted stones. The ablation probe and lithotripsy mechanism may make this technique less invasive, painless, and possibly an easy outpatient procedure. We have studied the mechanism of ablation and lithotripsy leading to the elimination of stones.

The purpose of this research is to study the features and parameters of the femtosecond laser useful for the efficacy of laser lithotripsy. Multi-pulse actions are analyzed. The plasma associated with the crater formed in the stone was also analyzed.

Keywords: stone crater, femtosecond laser, surgery, pain relief, laser

INTRODUCTION

Gallbladder stones cause a great pain in patients because of the mechanical disturbance to the surrounding tissue. It is of considerable importance to surgically remove larger stones and eventually prevent the subsequent growth of other stones which will cause further unnecessary pain. It is of interest to know the composition of the gallbladder stones and possible mechanism for their destruction especially if we want to use a powerful laser for the lithotripsy [1-3]. Studies of interaction of laser light with tissue and other materials has paved the way of laser-based lithotripsy [4-11]. Therefore, lithotripsy became a promising technique for kidney and gall bladder stone destruction [12-15]. For this purpose, different kind of lasers such as Nd-Yag, Eximer –Dye, Nd-YAG and Ho: YAG laser have been applied. Each of them seems to have advantages and

disadvantages [16-19]. However, it has been shown that Ho: Yag laser to be most useful for laser lithotripsy [20-26]. Later on, application of ultra-fast laser such as femtosecond laser, Fused logic and smart communication system is shown to be useful as well [27-32]. In this case enormous energy is concentrated on the target giving rise to formation of plasma, plume, shock waves and other phenomena constituting the dynamics and mechanisms associated with lithotripsy. When concentrated energy of laser is low, it means is low fluency or intensity, the multiphoton excitation could occur. However, due to low intensity of laser light, no destruction of the stone or removal of its material will take place.

On the other hand, when incident laser light is of high intensity, the number of excited electrons will increase reaching a density higher than a critical value. In this case a hot carrier absorption will occur and removal of material or destruction efficiency associated with ablation will be increased.

In order to study the mechanism and efficacy of laser lithotripsy, the action of a one single laser pulse and many pulse action, is studied in our work. When many pulses are applied, beside laser/mater interaction some other associated processes take place. For distinguishing pure interaction of laser light with matter only one pulse was applied at the beginning of our research. In this case of low amount of energy introduced, only electron excitation is performed and there is no interaction of light with the products due to ablation.

Experimental setup and procedure are presented in the next section. The femtosecond laser system is described. The collimation of the laser beam, its delivery to the stone and detection system is described.

Results and discussion are presented in two distinctive sections. Destruction of the stone is studied based on the ablation process or analysis of the formed craters due to action of the femtosecond laser power. The size of the crater formed and the role of the number of the laser pulses and their power is also evaluated.

The research approached as well the action of a single femtosecond laser. Qualitative analysis of the plasma that contributes to the ablation process corresponding pressure released on the liquid in the vicinity to the stone is correlated with the values of the power of the pulse applied. The image of plasma is recorded by a CCD camera and the pressure generated on the liquid

surroundings is recorded by hydrophones placed at the vicinity of the stone and immerses in the liquid.

The ablation process and lithotripsy is reached by application of many pulses of the femtosecond laser. The number of the pulses, their power related to the corresponding formed craters are presented later on.

EXPERIMENTAL

The femtosecond laser system used in the experiment contains 4 units, as shown in Fig.1. The incident pump laser light at 532 nm (15 W, Millennia, Spectra-Physics), is introduced to a Ti-sapphire mode-locked femtosecond laser with an output wavelength at 800 nm, a pulse duration of 120 fs and a repetition rate of 80 MHz (Tsunami, Spectra Physics). The desired fs-laser pulse output power is very low, in the range of nJ energy/per pulse. Therefore, the fs-laser beam from Tsunami is fed into the chirped pulse amplification system (Spitfire Pro, Spectra-Physics), operating at the same wavelength of 800 nm and the same pulse duration of 120 fs, but with a repetition rate of 1 kHz. Spitfire Pro amplifier is optically pumped by the laser light at 532 nm from the diode laser with a repetition rate of 1 kHz, as shown in Figure 1. The amplified laser beam is finally recompressed reaching a final output at a power of about 1.2 mJ/per pulse. The diameter of the amplified fs laser beam was of 8 mm, and as such was used in the present experiment.

A small portion of the laser output coming from the aperture was directed to an optical auto correlator using a cover plate for measuring the pulse width. The main portion of laser light was delivered through an electronic shutter (Newport Model 845 Digital Shutter Controller) hitting on the sample surface. The shutter is used to control the number of pulses reaching the sample. A beam expander in reverse mode was placed in between the cover plate and shutter for reducing the beam size to half of its original size (from 8 mm to 4 mm). An optical lens with a focal length of 100 mm was used for focusing the laser radiation onto the sample. The aberration free diameter at the focal point was calculated to be $21.5 \mu\text{m}$. The energy per pulse measured after the optical elements, just before action on the sample surface, it was 9 mJ. The power density was estimated to approximately 10^{14} W/cm^2 . This confirms the sufficient condition for plasma induced ablation mechanism.

A stone previously extracted operatively from the human gall bladder was polished perfectly and kept in de-ionized water for about 24 hrs before conducting the experiments. The sample was submerged in water by using a stone holder such that only a very little amount of water was maintained above the stone surface where the laser was hitting, as shown in Figure 1. The laser light was hitting on the stone surface from top and the plasma is formed during the laser action. The plasma was recorded using a CCD camera from the side. At the same time a hydrophone signal for a single shot pulse was recorded by immersing it in the beaker with de-ionized water where the sample was held. The shock wave pressure formed due to plasma expansion was captured by the hydrophone (Model ITC-1089D) and it was recorded using an oscilloscope. After finishing the experiments, the sample calculus was dried out in air. The craters formed as a result of laser ablation were viewed by means of the optical microscopy. The diameter and the depth of craters were measured using a microscope. The changes in the crater morphology and ablation rates at different number of pulses and power of the laser was thus studied. By knowing the depth and the diameter of the crater, we could estimate the volume of the crater or eventually the material contained.

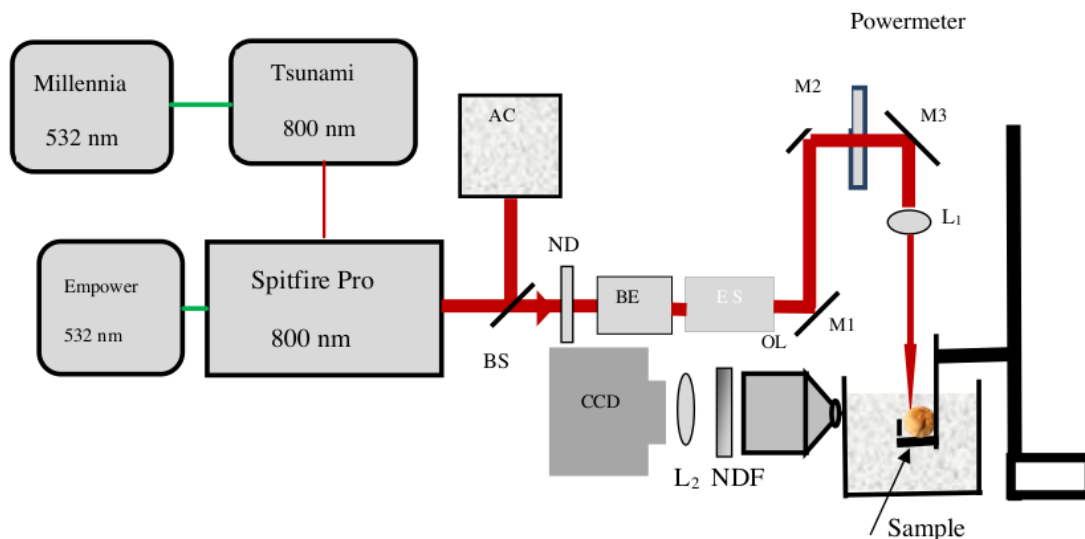


Fig 1: Schematic diagram of the experimental set-up of the laser ablation used in this study. AC: Auto-Correlator, BE: Beam Expander, OL: Objective lens, NDF: Neutral density filter.

To study the effect of multiple pulses on the sample calculus, different numbers of pulses are applied normally to the polished sample surface at 1 KHz repetition rate. The crater size variations with number of pulses were thus studied. The effect of different power at a particular number of pulses was also studied and it is imaged using neutral density filters having different optical densities

RESULTS

Formation of craters by power action of the femtosecond laser

Femtosecond laser of 120 femtoseconds ($1\text{fs} = 10^{-15}$ seconds) pulse duration and the repetition rate of 80 MHz, with a high-power density is applied, achieving energy much greater than the damage threshold of the stone material.

The power density applied, was measured to be of the order of 10^{14} W/cm² which is higher than the threshold (10^{11} W/cm²) required for plasma induced ablation of materials. This confirms that light emitted from a femtosecond laser is capable of plasma mediated ablation mechanism. The laser beam waist was determined to be 21 microns by assuming that femtosecond laser beams have Gaussian distribution. Here we study the material on the surface or craters formed after the action of laser light.

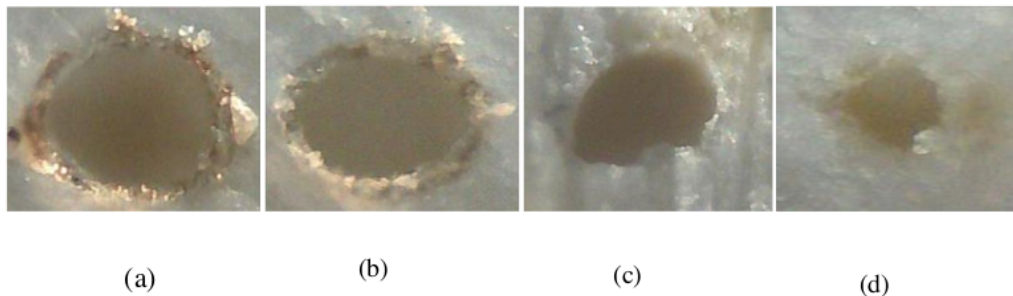


Fig. 2. Optical microscopy images of the femtosecond ablation craters obtained with: (a) 60 000 pulses (b) 50 000 pulses (c) 30 000 pulses (d) 10 000 pulses. Scale bar 100 μm

Analysis of the craters

In Figure 2 we show the craters formed due to action of the pulsed laser power. We have measured the size and the depth of the craters and we have evaluated results when different number of pulses and different pulse powers were applied.

Table 1. Diameter, depth and volume of ablation craters for 50 000 pulses at different laser power.

No	No of pulses 50000								
	Diameter (μm)			Depth (μm)			Volume(μm^3)[$1/3 \pi r^2 h$]		
	900 mW	700 mW	500 mW	900 mW	700 mW	500 mW	900 mW	700 mW	500 mW
1	230	210	200	4250	3600	3150	53.85 $\cdot 10^6$	41.56 $\cdot 10^6$	32.98 $\cdot 10^6$

In Table 1, the data obtained for the diameters and the depths of a craters, for the applied laser pulse powers of: 900mW, 700mW and 500mW, are shown. Assuming that the crater has a conical shape, using the sizes of diameters of the crater, for different power, and data measured using a microscope, the volumes for different power values are determined. The values are shown in Table 1 as well.

Table 2. Diameter, depth and volume of ablation craters for 60000 pulses at different laser power.

Using the number of pulses applied	No	No of pulses 60000								
		Diameter (μm)			Depth (μm)			Volume(μm^3)		
		900 mW	700 mW	500 mW	900 mW	700 mW	500 mW	900 mW	700 mW	500 mW
1	250	240	230	4800	4100	3800	78.53 $\cdot 10^6$	61.82 $\cdot 10^6$	52.62 $\cdot 10^6$	

powers, for different pulse numbers.

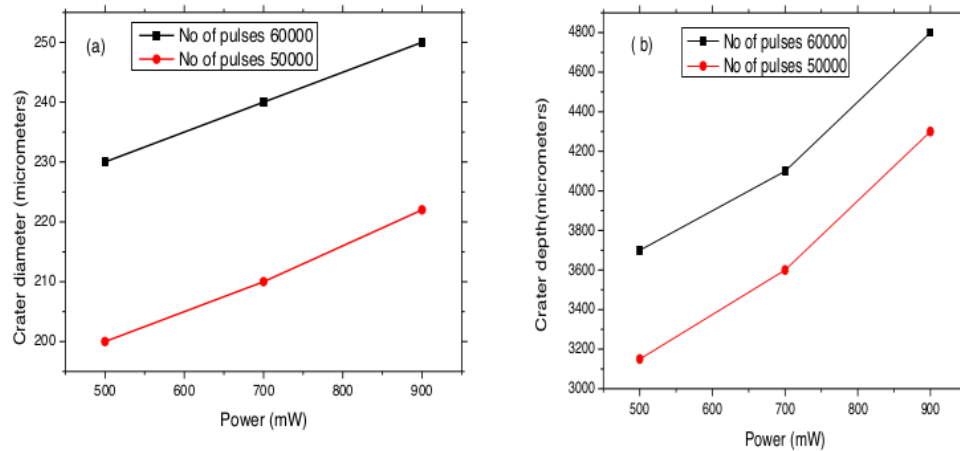


Fig. 3. (a) Diameter values of crater versus power applied and (b) the depth values versus powers. In both cases 60 000 and 50 000 pulses are applied.

It can be seen that the size of the depth increases linearly when the powers increase, as shown in Figure 3 (a). A big increase of the diameter is shown when the number of pulses is increased from 50 000 to 60 000 pulses.

On the other hand, the increase of the depth with power values, in Figure 3 is shown for 50 000 and 60 000 pulses as well. It is obvious a quantitative difference between these two cases. For the first case, the function of diameter sizes versus power remains almost a linear function for different number of pulses. However, the graph representing the depth of the crater versus the power seems to be different, as shown in Figure 3 (b). While the powers lower than 700 mW it shows a linear behavior, at this point a kink has appeared. Namely, for the power higher than 700 mW, an increase of the slope is shown for both numbers of pulses, for 60 000 and 50 000 pulses, respectively. The cause for this phenomenon is a subject of the ongoing research. However, this is a new information that could be used for the efficacy of the laser lithotripsy. Namely, here is shown that by for the same number of pulses and power introduced, the depth of the craters is increased faster.

In order to understand formation of craters due to action of laser power or the mechanism of ablation process several experiments are conducted. Firstly, the plasma due to a single pulse action and corresponding pressure generated due to shock wave formation is studied. Then the role of

plasma generated due to multiple pulses radiation for different powers is evaluated. Finally, we have studied the plasma generated using spectroscopic technique.

The power action and formation of plasma due to multi-pulse ablation

Here we study qualitatively the distribution of plasma and corresponding crater formed on the stone due to multi pulse femtosecond laser action. Results are shown in Figure 4.

The system of the panels shown in Figure 4 is ordered on three rows obtained for different introduced laser power. The row a) corresponds to a power of 500 mW, row b) corresponds to a power of 700 mW and c) represents the case when the laser power was 900 mW. The left column of this system of panels shows the crater images obtained for different powers. Middle column represents the corresponding images of plasma for different powers. The right column shows the processed version of the images of the middle column. All the crater and other images are obtained for the same number of 60000 applied pulses. Here the plasma mediated ablation for different introduced powers is evaluated.

The spatial distribution of plasma is shown in Figure 4. The white shapes, of the images of the two upper cases, of the middle columns, shows a relatively well concentrated plasma with a considerably similar shape. However, the corresponding panels on the right columns representing the processed images, have different distribution of isotherms. Surprising is the size of the plasma core of the image corresponding to the incident light power of 500 mW. This seems to be bigger or the same size compares to the case when incident power was of greater value 700mW. However, the crater size, shown in the middle of the first column, corresponding to the latter case, when higher (700 mW) power was applied, is of bigger size. For this case, the processed image seems to have concentric pattern of isotherms is wider with greater number of rings.

In case when the incident power is 900mW, the generated plasma is wider, shown in the middle column, and it has the concentrated uniform core, shown in the right column, the third row. In this case the edge of the crater formed by ablation is shown to be less sharp than in case when the power of 700 mW is applied.

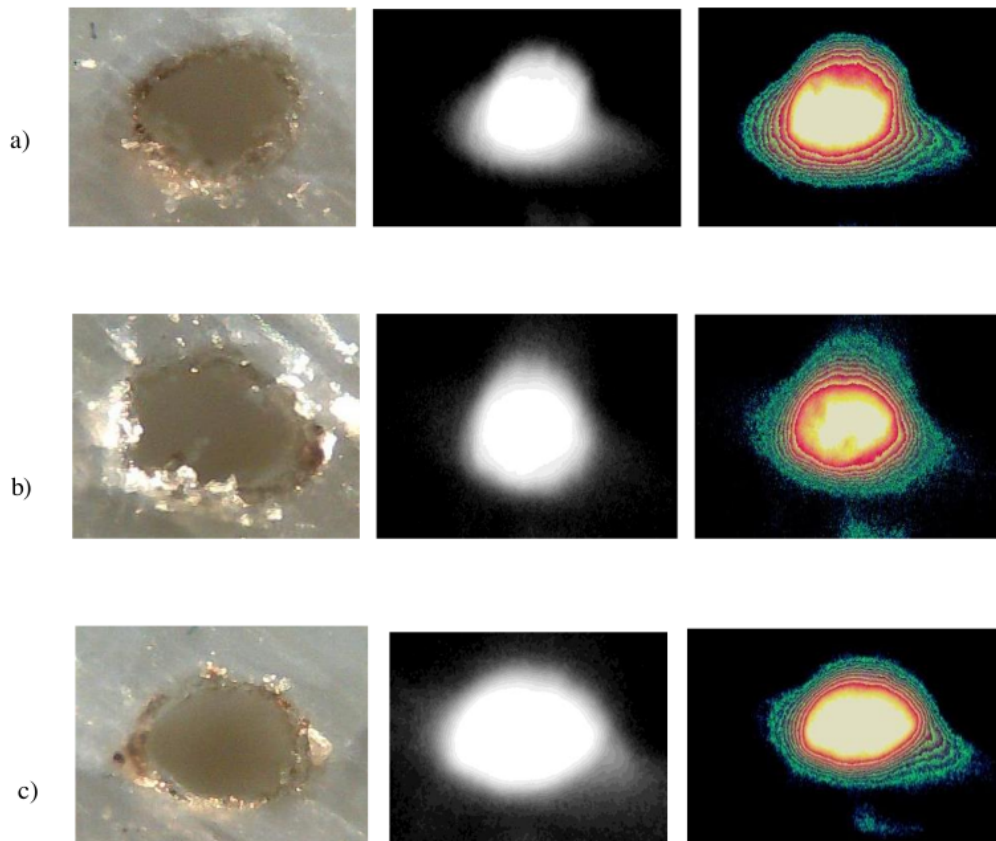


Fig. 4. Images of craters, plasma and computer processed images when 6000 pulses are applied. The first row denoted by a) corresponds to 500 mW power of each pulse, the rows b) and c) corresponds to the power of pulses of 700 mW and 900 mW respectively.

When the fluency or intensity applied, is higher and when multiple emission is applied, as shown in in case b) and c) of the Figure 4, an additional mechanism like hot carrier absorption occurs via electron-photon—electron interaction. This would lead the increase of efficiency of ablation.

For multiple-pulse irradiation the coulomb explosion that is the repulsion of positive ions in a volume formed after electron excitations, is not significant. In this case the main factor is the transient effect akin to the increase of ablation efficiency. Multi pulse action contributes to the lower threshold intensity and consequently increase the ablation dynamics when number of pulses and power action is increased. Therefore, the craters in case b) and c) greater indicating an increase of efficacy of ablation and laser-based lithotripsy.

DISCUSSION

The action of pulsed laser power on a gallbladder stone removes some material and makes a crater. By increasing the number of laser pulses and its power the volume of the crater is increased until the stone is destructed and eliminated. Therefore, the study of the crater and its size related to the number of pulses and their power would lead us to a desired efficacy and better strategy for laser lithotripsy.

While in case of action of a single femtosecond laser pulse a pure interaction of laser light with the matter takes place, in case of multi pulse action an integral dynamic of phenomena such as plume and plasma formation, shock wave generation and propagation will take place. These secondary phenomena will interact with the incoming laser light and will generate mechanisms and effects contributing to the lithotripsy. The mechanisms that mediate the femtosecond laser lithotripsy is not well understood. However, it is known that the plume and plasma formed plays a key role in mechanism of laser-based lithotripsy.

CONCLUSION

Medical technology in general and laser application in particular has modernized the surgery, diagnostics and therapeutic techniques. Laser energy delivered by an optical fiber to the stone inside the organism has been applied. However, investigation of the laser pulses, the length, power and frequency for the faster destruction, can lead to the better strategies, increase the robustness and make this technique painless and economically convenient.

In this study we applied femtosecond laser for destruction of the stones previously extracted by surgery from the human gallbladder. The crater formed by a chosen laser power and number of the pulses, as shown in Tables 1, 2, and Figure 3 are analyzed. Increase of the number of pulses is shown to be advisable, when the laser is used in vivo, for the lithotripsy. Figure 4 and processed images show the plasma action and distribution as an additional useful factor to the nominal laser pulse power applied.

References:

1. Wrobel R, Niay P, Bernage P, Blondeau JM, Ledee JJ, Brunetaud JM. Identification of Cholesterol Gallstones Using in Vitro Low-Fluence Laser-Induced Fluorescence Spectroscopic Analysis. *Appl Phys B*. 1990 Dec;51:458-464. doi: 10.1007/BF00329112.
2. Kim IS, Myung SJ, Lee SS, Lee SK, Kim MH. Classification and nomenclature of gallstones revisited. *Yonsei Med J*. 2003 Aug 30;44(4):561-70. doi: 10.3349/ymj.2003.44.4.561. PMID: 12950109.
3. Singh VK, Singh V, Rai AK, Thakur SN, Rai PK, Singh JP. Quantitative analysis of gallstones using laser-induced breakdown spectroscopy. *Appl Opt*. 2008 Nov 1;47(31):G38-47. doi: 10.1364/ao.47.000g38. PMID: 19122701.
4. Vogel A, Schweiger P, Asiyu M, Birngruber R. Intraocular Nd-YAG Laser surgery: light tissue interactions, damage range, and reduction of collateral effects. *IEEE J Quantum Electron*. 1990 Dec;26(12):2246-60. Available from: https://www.bmo.uni-luebeck.de/fileadmin/files/publications/Vogel__1990_IEEE_J_Quantum_Electron_Intraocular_Nd_YAG_laser_Surgery_Light-Tissue_Interaction__Damage_Range__and_Reduction_of_Collateral_Effects.pdf
5. Takayama K. Holographic interferometric study of shock wave propagation in two-phase media. In: Proc. 16th IST & W. Aachen. 1987. p. 52–61.
6. Nishioka NS, Levins PC, Marry SC, Parish JA, Anderson RR. Fragmentation of binary Calculi with tunable dye lasers. *Gastroenterology*. 1987 Aug;93(2):250-5. doi: 10.1016/0016-5085(87)91010-9.
7. Marafi M, Makdisi Y, Bhatia KS, Abdulalh H, Kokaj J. Laser ablation of gall bladder stones. *Spectrochim Acta A Mol Biomol Spectrosc*. 1999 Jun;55A(6):1291-6. doi: 10.1016/s1386-1425(98)00298-4.
8. J M Teichman¹, G J Vassar, J T Bishoff, G C Bellman, J Urol. 1998 Jan;159(1):17-23. doi: 10.1016/s0022-5347(01)63998-3.
9. Ell C, Hochberger J, Müller D, Zirngibl H, Giedl J, Lux G, Demling L. Laser lithotripsy of gallstone by means of a pulsed neodymium-YAG laser--in vitro and animal experiments. *Endoscopy*. 1986 May;18(3):92-4. doi: 10.1055/s-2007-1018339.

10. Thomas, S, Engelhardt R, Meyer W, Brinkmann R, Hofstetter A G, Laser induced shock wave lithotripsy. *Berichte der Bunsengesellschaft für physikalische Chemie*. März 1989; 2:36-42. <https://doi.org/10.1002/bbpc.19890930314>
11. Ready J. *Effects of high-power laser radiation*. New York: Academic Press; 1971, Academic Press; 1st edition (September 11, 1971) ISBN-10 : 0125839502, ISBN-13 : 978-0125839501.
12. Ponchon T, Gagnon P, Valette PJ, Henry L, Chavaillon A, Thieulin F. Pulsed dye laser lithotripsy of bile duct stones. *Gastroenterology*. 1991 Jun;100(6):1730-6. doi: 10.1016/0016-5085(91)90676-c.
13. M Delhay¹, A Vandermeeren, M Baize, M Cremer. Extracorporeal shock-wave lithotripsy of pancreatic calculi. *Gastroenterology*. 1992 Feb;102(2):610-20. doi: 10.1016/0016-5085(92)90110-k.
14. Rene. G. Laser fragmentation of pancreatic stones. *Endoscopy* 1991; 23: 166-70.
Renner IG. Laser fragmentation of pancreatic stones. *Endoscopy*. 1991 May;23(3):166-70. doi: 10.1055/s-2007-1010648.
15. Flowers BF, Saslawsky MJ, Mathes GL, Tonkin AK. Use of the pulsed dye laser and ultrasonic lithotripter for removal of multiple intrahepatic gallstones. *Surg Gynecol Obstet*. 1990 May;170(5):443-4.
16. Teng P, Nishioka NS, Rox Andersen R, Deutsch TF. Optical studies of pulse laser fragmentation of biliary calculi. *Appl Phys B*. 1987 Feb;42:73-8. doi: 10.1007/BF00694813.
17. Rink K, Delacrétaz G, Salathé RP. Fragmentation process induced by microsecond laser pulses during lithotripsy. *Appl Phys Lett*. 1992;61:258-60. doi: 10.1063/1.107961.
18. Praneeth Kudaravalli, Bilal Aslam, Moamen Gabr. A Review of Lithotripsy Applications in Gastroenterology. *Frontiers in Endoscopy, Series #46, October 2018 • Volume XLII, Issue 10*.
19. Neuhaus H. Fragmentation of pancreatic stones by extracorporeal shock wave lithotripsy. *Endoscopy*, 1991 May;23(3):161-5. doi: 10.1055/s-2007-101064.
20. K Trauner¹, N Nishioka, D Patel. Pulsed holmium:yttrium-aluminum-garnet (Ho:YAG) laser ablation of fibrocartilage and articular cartilage, *Am J Sports Med*. 1990 May-Jun;18(3):316-20. doi: 10.1177/036354659001800316.
21. Marafi M, Kokaj J, Bhatia K, Makdisi Y, Mathew J. Laser spectroscopy and imaging of gallbladder stones, tissue and bile. *Opt Laser Eng*. Volume 45, Issue 1, January 2007, 191-197. <https://doi.org/10.1016/j.optlaseng.2006.03.014>
22. Kokaj J, Makdisi Y, Marafi M, Bhatia K. High speed imaging and optical correlation for Laser-induced shock-wave lithotripsy. *Optik* 1999; 110; 497-540.
23. Kokaj j, Mathews J. Imaging and optical correlation used for guided laser lithotripsy. *Opt*

- Laser Tecnnol 2004; 36: 44108. DOI: 10.1016/j.optlastec.2003.12.012
24. Tipmongkonspil S, Kumar B, Kokaj J. Equivalence of two approaches to the design of OR correlation filter: Application in Laser Lithotripsy. SPIE 2000; 4043; 110: 497-540. DOI:10.1117/12.381590
 25. Kokaj J, Marafi M, Mkdisi K, et al. A smart Ho: YAG laser lithotripter using correlation, SPIE 1998; 3386: 301-10. DOI:10.1117/12.304776
 26. Kokaj J, Marafi M, Mathew J. Optical investigation of dynamics of phenomena of laser-based lithotripsy. Optics and Lasers in Engineering 2008; 46: 535-540. DOI:10.1016/j.optlaseng.2008.02.006
 27. Cavalleri te al. Femtosecond x-ray studies of phase transition dynamics in strongly correlated solids. Phys Rev Lett 2001; 87: 237-401. DOI:<https://doi.org/10.1103/PhysRevlett.87.237401>
 28. Gattass R, Mazur E. Femtosecond laser micromachining in transparent materials. [Nature Photonics](#) 2(4):219-225; 2008. DOI:[10.1038/nphoton.2008.47](https://doi.org/10.1038/nphoton.2008.47)
 29. Kabashin A, Meunier M. Sunthesis of colloidal nanoparticles during femtosecond laser ablation of gold in water, J Appl Phys 2004; 94: 7941-7943. DOI:[10.1063/1.1626793](https://doi.org/10.1063/1.1626793)
 30. Gamaly EG, Rode AV, Tikhonchuk V T, Luther-Davis B. Ablation of solids by femtosecond lasers: Ablation mechanism and ablation thresholds for metal and dielectrics, Phys Plasmas February 2001-9(3) DOI:[10.1063/1.1447555](https://doi.org/10.1063/1.1447555)
 31. Kokaj Agon, Maluku Betim. A Communication System For Smart Network Systems, [IFAC-PapersOnLine](#). Volume 54, Issue 13, 2021, Pages 68-71. <https://doi.org/10.1016/j.ifacol.2021.10.420>
 32. Bajrami X, Demaku A, Kokaj A, Published in Mediteran Conference, June 12 2016 Comuter science engineering Comp ID 45753928. DOI:10.1109/MECO.2016.7525739.